NDT
Nephrology Dialysis Transplantation

Original Article

Indoxyl sulphate promotes aortic calcification with expression of osteoblast-specific proteins in hypertensive rats

Ayinuer Adijiang[1], Sumie Goto[2], Satsuki Uramoto[2], Fuyuhiko Nishijima[2] and Toshimitsu Niwa[1]

[1]Department of Clinical Preventive Medicine, Nagoya University Hospital, Nagoya, Japan and [2]Biomedical Research Laboratories, Kureha Co., Tokyo, Japan

Abstract

Background. Stage 5 chronic kidney disease (CKD) is associated with enhanced aortic calcification. The aim of this study was to determine if the administration of indoxyl sulphate (IS), a uraemic toxin, stimulates the progression of aortic calcification.

Methods. The rat groups consisted of (i) Dahl salt-resistant normotensive rats (DR) with intake of 0.3% salt, (ii) Dahl salt-sensitive hypertensive rats (DS) with intake of 2.0% salt and (iii) Dahl salt-sensitive hypertensive IS-administered rats (DS-IS) with intake of 2.0% salt and 200 mg/kg of IS in water. After 30 weeks, their aortic and kidney tissues were excised for histological and immunohistochemical analyses.

Results. Severe vascular calcification was observed by von Kossa staining in the arcuate aorta of all the DS-IS rats, but hardly in DS or DR rats. Immunohistochemistry demonstrated that osteopontin, core binding factor 1 (Cbfal), alkaline phosphatase (ALP), osteocalcin, IS and organic anion transporter (OAT) 3 were colocalized in the cells embedded in the aortic calcification area of DS-IS rats. Wall thickness was significantly increased in arcuate, thoracic and abdominal aortas of DS-IS rats compared with DS and DR rats. DS-IS rats showed significantly increased extent of glomerular hypertrophy, mesangial expansion, Masson's trichrome-positive tubulointerstitial area and glomerular and tubulointerstitial expression of transforming growth factor-ßl as compared with DS and DR rats.

Conclusions. IS induced aortic calcification with expression of osteoblast-specific proteins and aortic wall thickening. IS is not only a nephrotoxin but also a vascular toxin, and may contribute to the progression of aortic calcification in stage 5 CKD patients.

Keywords: aortic calcification; indoxyl sulphate; organic anion transporter; osteopontin; uraemic toxin

---

Correspondence and offprint request to: Toshimitsu Niwa, MD, PhD, Nagoya University Hospital, Department of Clinical Preventive Medicine, 65 Tsurumai-cho, Showa-ku, Nagoya 466-8560, Japan. Tel: +81-52-744-1980; Fax: +81-52-744-1954; Email: tniwa@med.nagoya-u.ac.jp

Introduction

Indoxyl sulphate (IS) is a uraemic toxin that accelerates the progression of chronic kidney disease (CKD) [1,2]. It is derived from dietary protein. A part of protein-derived tryptophan is metabolized into indole by tryptophanase by intestinal bacteria, such as *Escherichia coli.* Indole is absorbed into the blood from the intestine, and is metabolized to IS in the liver. IS is normally excreted into urine. In uraemia, however, the reduced renal clearance of IS leads to elevated serum levels of IS. Serum IS levels are increased in patients with CKD [3,4]. Administration of IS and its precursor, indole, to 5/6 nephrectomized rats increased glomerular sclerosis in the remnant kidney with a decline in renal function [4,5]. Furthermore, IS stimulated transcription of genes related to renal fibrosis, such as transforming growth factor (TGF)-ß1, tissue inhibitor of metalloproteinases (TIMP) 1 and pro-αl collagen [6,7]. The induction of nephrotoxicity by IS is mediated by organic anion transporters (OATs), such as OAT types 1 and 3 in the basolateral membrane of renal proximal tubular cells [8]. IS induces free radical production by renal tubular cells, and activates nuclear factor-κB, which, in turn, upregulates expression of plasminogen activator inhibitor 1 [9].

Cardiovascular disease accounts for 40–50% of deaths in dialysis populations. Cardiovascular disease mortality in haemodialysis and peritoneal dialysis patients is much higher especially in younger age categories than age- and sex-matched controls without CKD [10,11]. Vascular calcification plays a vital role in the development of cardiovascular morbidity and subsequent increased mortality. Vascular calcification affects both vascular intima and media layers and its mechanism remains poorly understood. In addition to traditional cardiovascular risk factors, hyperphosphataemia, calcium overload, increased oxidized low-density lipoprotein cholesterol, uraemic toxins, increased oxidative stress, hyperhomocysteinaemia, haemodynamic overload and dialysate-related factors may also play a role [12].

IS inhibits endothelial proliferation and wound repair [13]. Recently, it has been reported to stimulate proliferation of rat vascular smooth muscle cells [14]. These

in vitro experiments suggest that IS may play a role in the dysfunction of endothelial and vascular smooth muscle cells in CKD patients. We hypothesized that IS is a uraemic toxin accelerating progression of vascular calcification.

In this study, we determined if administration of IS accelerates aortic calcification *in vivo*.

Methods

In vivo experimental design

Dahl salt-resistant rats (Dahl-Iwai R, *n* = 5) and Dahl salt-sensitive rats (Dahl-Iwai S, *n* = 20) were purchased at 5 weeks of age from Japan SLC, Inc. (Hamamatsu, Shizuoka, Japan), and were fed powder rat chow (CE-2, Clea, Tokyo, Japan) for 1 week. Then, the Dahl-Iwai R rats were fed the chow (CE-2) with a low-salt (0.3% NaCl) intake in water, and Dahl-Iwai S rats were fed the chow (CE-2) with a high-salt (2.0% NaCl) intake in water. At 7 weeks of age, Dahl-Iwai S rats spontaneously developed hypertension with systolic blood pressure (BP) more than 140 mmHg. Then the rats were divided into two groups: control rats and IS-administered rats. Thus, the rat groups consisted of (i) Dahl salt-resistant normotensive rats (DR, *n* = 5) with an intake of 0.3% NaCl in water, (ii) Dahl salt-sensitive hypertensive control rats (DS, *n* = 10) with an intake of 2.0% NaCl in water, (iii) Dahl salt-sensitive hypertensive IS-administered rats (DS-IS, *n* = 10) with an intake of 2.0% NaCl and 200 mg/kg of IS (Alfa Aesar, Lancashire, England) in water, for 30 weeks. BP was measured using the tails of the rats with a pneumatic cuff and a sphygmomanometer for small animals (UR-5000, Ueda Avancer Co., Tokyo, Japan). Because five DS rats and four DS-IS rats have died during the study, the remaining five DS rats and six DS-IS rats were analysed. Although the cause of death in the DS and DS-IS rats is unknown, it may be related with hypertension and overhydration due to the intake of 2.0% NaCl. None of the DR rats died because they were normotensive and took 0.3% NaCl. At the end of the experiments, the rats were anaesthetized and their aortic tissues and kidney tissues were excised for histological and immunohistochemical analyses in conformity with national and international laws for the care and use of laboratory animals.

Analytical procedures

Serum and urine levels of IS were measured by high-performance liquid chromatography (HPLC) according to the modified method of our previous papers [15,16]. In the papers, we reported a rapid assay for IS as total concentration without prior deproteinization of serum samples by internal surface reverse-phase liquid chromatography. The HPLC system (Shimadzu, Kyoto, Japan) consists of an auto-injector (SIL-10AD) at 4°C, a degasser (DGU-12A), a pump (LC-10AD), a column oven at 35°C (CTO-10AC), a column (Shiseido Capsule Pack MF Type SG80, 4.6 mm × 150 mm, 5 μm), a fluorescence detector (RF-10A XL), a system controller (SCL-10AP) and software (CLASS-VP). Serum sample was analysed for 10 min with a mobile phase, 5% tetrahydrofuran/0.1M KH_2PO_4

(pH 6.5) at a flow rate of 1 ml/min and a fluorescence detection (Ex. 295 nm and Em. 390 nm). IS is dissociated from albumin in the mobile phase containing tetrahydrofuran, and separated from the other components by the internal-surface reverse-phase of microparticles in the column. The Shiseido Capsule Pack MF column is designed for direct injection of serum samples which tolerates 800 injections. Serum proteins elute freely though the column without any retention. Thus, the column does not require deproteinization procedure for serum.

Serum samples were centrifuged at 1000 *g* for 20 min at 4°C, and the supernatant serum (10 μl) was injected into the HPLC system. An internal standard was not used for the assay. A calibration line was generated with serum standards containing IS at final concentrations of 0.00627 to 12.6 mg/dl, and the square of correlation coefficient (R^2) of the line was 0.9999. The limit of quantification was from 0.06 to 12 mg/dl. Coefficients of variation (CV) (*n* = 5) for the intra-assay variability of IS at concentrations of 0.126 mg/dl and 2.51 mg/dl were 0.84%, and 0.24%, respectively, and their accuracy values were 103.2% and 102.3%, respectively. CV values (*n* = 5) for the inter-assay variability of IS at concentrations of 0.126 mg/dl and 2.51 mg/dl were 2.2% and 1.5%, respectively, and their accuracy values were 100.7% and 101.7%, respectively. CV (*n* = 5) for the stability of IS at a concentration of 2.51 mg/dl kept at room temperature for 2 h was 0.3%, and its accuracy was 104.2%. CV (*n* = 5) for the stability of IS at a concentration of 2.51 mg/dl kept at −40°C for 180 days was 1.8%, and its accuracy was 96.3%. According to the standard addition method, quality control serum samples in which IS was added at different concentrations (standard concentration), were analysed five times. The average measured concentration of IS was calculated by considering endogenous concentration of IS. Accuracy was calculated as follows:

$$\text{Accuracy (\%)} = (\text{average measured concentration}/ \text{standard concentration}) \times 100$$

Creatinine and blood urea nitrogen (BUN) levels were measured using a Beckman Synchron CX3 auto-analyser. Urine protein was measured using the pyrogallol red method (micro TP test, Wako Pure Chemical Industries, Ltd., Osaka, Japan).

Tissue preparation and histology

Aortic tissues were dissected, fixed in formalin and processed for paraffin embedding. Then, the tissues were stained by haematoxylin and eosin (H&E), and by von Kossa to detect calcification. The thickness of aortic wall was measured by morphometry of H&E-stained aortic sections. The pictures of aortic tissue sections were taken by a digital camera (DN100, Nikon, Tokyo, Japan), and the thickness of aortic wall was measured in five different areas per aortic section using an image analysis computer program (NIH Image 1.62). The average value of five measurements was considered representative of each rat. Calcification area was measured in two von Kossa-staining sections of the arcuate aorta for each rat using the image analysis computer program [17].

Kidney tissues were dissected, fixed in formalin and processed for paraffin embedding, and thin sections were stained by periodic acid-Schiff (PAS) and Masson's trichrome (MT). For measurement of glomerular area and mesangial area, the pictures of PAS staining were taken on 10 different glomeruli per section by a digital camera (DN100, Nikon), and displayed on a computer board using the software of Adobe Photoshop® 6.0. The glomerular area and PAS-positive area (identical with mesangial area) in the same glomerulus were determined by Adobe Photoshop®, and measured using NIH Image 1.62. For measurement of interstitial fibrosis, the pictures of MT staining were taken on 10 different sections in the renal cortex by the digital camera. MT-positive area except glomeruli was determined by Adobe Photoshop®, and measured using NIH Image 1.62. The average value of 10 measurements was considered representative of each rat.

Immunohistochemistry

Paraffin-embedded tissue sections were deparaffinized in xylene, and rehydrated in ethanol. Deparaffinized sections underwent a microwave treatment in citrate buffer (10 mmol/1, pH 6.0) twice for 5 min, and rinsed in tap water to retrieve antigens. Endogenous peroxidase was inhibited with 0.3% H_2O_2 methanol for 10 min, followed by a rinse in phosphate buffered saline. Sections were blocked by 10% serum (Nichirei Co, Tokyo, Japan) at room temperature for 30 min. Immunostaining was processed according to the streptavidin–biotin complex (SABC) method.

For immunostaining of osteoblast-related proteins, such as osteopontin, alkaline phosphatase (ALP) and osteocalcin in the aortas, mouse monoclonal anti-osteopontin (1:1000, No. 01-20002, American Research Products, Inc, Belmont, MA, USA), anti-ALP (1:50, No. MAB1448, R&D Systems, Inc, Minneapolis, MN, USA) and anti-osteocalcin (1:100, No. a1/3420, Abcam, Cambridge, UK) antibodies were used as the primary antibodies, respectively. The slides were incubated with the secondary antibody (biotin-labeled rabbit anti-mouse IgG antibody, Nichirei Co) at room temperature for 30 min, and then with peroxidase-conjugated streptavidin (Nichirei) at 37°C for 30 min. After another wash with PBS, peroxidase activity was detected by reaction with 3,3′-diaminobenzidine tetrahydrochloride (DAB tablet, Merck KGaA, Darmstadt, Germany; 30 mg/ml, containing 0.03% H_2O_2) as the chromogen. Finally, sections were counterstained by 1% methylene green, dehydrated and mounted. Staining without the primary antibody was used as a negative control.

For immunostaining of Cbfal in the aortas, a polyclonal anti-Cbfal antibody (1:100, No. M-70, sc-10758, Santa Cruz Biotechnology, Inc, CA, USA) was used. The slides were incubated with the secondary antibody (biotin-labeled goat anti-rabbit IgG antibody, Nichirei Co). Cbfal expression in vascular smooth muscle cells is an early definitive marker of osteoblastic differentiation, and controls the expression of osteopontin, ALP and osteocalcin.

For immunohistochemistry of IS, rOATl and rOAT3 in the aortas, a mouse monoclonal anti-IS antibody (1:100), a rabbit polyclonal anti-rOATl antibody (1:20) and a rabbit polyclonal anti-rOAT3 antibody (1:100) that were pro-

duced in our laboratory were used. The characterization of the monoclonal anti-IS antibody was described previously [18], and the specificity of the rabbit polyclonal anti-rOATl and anti-rOAT3 antibodies was described elsewhere [19,20].

For immunohistochemistry of smooth muscle actin (SMA) in the aortas, a mouse monoclonal anti-SMA antibody coupled with horseradish peroxidase (1:1, No. U7033, Dako Cytomation, Glostrup, Denmark) was used. For immunohistochemistry of macrophages, a mouse monoclonal anti-CD68 antibody coupled with horseradish peroxidase (1:1, No. U7029, Dako Cytomation) was used.

For immunostaining of TGF-ßl in the kidneys, sections were treated with diluted proteinase K solution (0.01 mg/ml) at 37°C for 10 min before staining, and then stained using a polyclonal anti-TGF-ßl antibody (1:20, Santa Cruz Biotechnology). Ten glomeruli and 10 tubulointerstitial areas per section were randomly selected on the kidney cortex, and TGF-ßl-positive areas in glomeruli and tubulointerstitium were determined by Adobe Photoshop®, and measured using NIH Image 1.62. The average value of 10 measurements was considered representative of each rat.

Statistics

All quantitative data are presented as mean ± SE. To compare values among the three groups, analysis of variance (ANOVA) was applied and Fisher's least significant difference (LSD) test was used. Results were considered statistically significant when the *P* value was less than 0.05.

Results

Laboratory parameters

Table 1 summarizes the time course of laboratory parameters in DR, DS and DS-IS rats. As compared with DR rats, DS rats showed a significant increase in systolic BP and serum and urine levels of Na and Cl, and a significant decrease in diet, body weight, creatinine clearance, serum and urine levels of K and urine creatinine. As compared with DS rats, DS-IS rats showed significantly increased serum and urine levels of IS. However, there were no significant differences in systolic BP, BUN, serum creatinine, creatinine clearance, serum Ca, serum P, total cholesterol and HDL cholesterol between DS and DS-IS rats.

Figure 1 shows the time course of systolic BP and serum IS in DR, DS and DS-IS rats. Both DS and DS-IS rats showed significantly increased systolic BP as compared with DR rats, although there was no significant difference in systolic BP between DS and DS-IS rats. Serum IS levels were significantly increased in DS-IS rats as compared with DS and DR. Thus, administration of IS to DS rats significantly increased serum levels of IS, although systolic BP was kept as high as in the DS rats.

Quantification of aortic calcification and aortic thickness

Figure 2 shows H&E and von Kossa staining pictures of the arcuate aorta in DR, DS and DS-IS rats. Calcification was

Table 1. Time course of laboratory parameters in DR, DS and DS-IS rats

	DR					DS					DS-IS				
Week	0	9	17	25	30	0	9	17	25	30	0	9	17	25	30
n	5	5	5	5	5	5	5	5	5	5	6	6	6	6	6
Diet (g/day)	23.0 ± 0.4[d]	22.4 ± 0.8[b]	21.6 ± 1.1[b]	22.8 ± 0.6[b]	25.5 ± 0.6[b]	20.0 ± 0.7	17.7 ± 0.8	17.5 ± 0.9	17.6 ± 0.6	15.1 ± 1.5	20.5 ± 0.6	20.5 ± 0.9[a]	18.4 ± 0.2	18.3 ± 1.2	15.3 ± 1.8
BW (g)	433 ± 4[d]	515 ± 9[d]	571 ± 13[d]	599 ± 14[d]		342 ± 9	387 ± 14	419 ± 14	417 ± 13		347 ± 6	401 ± 9	435 ± 7	427 ± 10	
Systolic BP (mmHg)	127 ± 2[d]	126 ± 1[d]	118 ± 3[d]	121 ± 2[d]		158 ± 5	170 ± 4	173 ± 2	175 ± 2		157 ± 3	172 ± 4	182 ± 4	179 ± 9	
Heart rate (/min)	374 ± 4	360 ± 3	361 ± 6	355 ± 9		380 ± 20	358 ± 13	369 ± 14	362 ± 8		387 ± 5	382 ± 12	388 ± 10	369 ± 18	
S-IS (mg/dl)	0.27 ± 0.03[d]	0.25 ± 0.02	0.16 ± 0.01	0.17 ± 0.03	0.08 ± 0.01	0.08 ± 0.01	0.12 ± 0.02	0.10 ± 0.01	0.09 ± 0.02	0.10 ± 0.03	0.13 ± 0.02	1.64 ± 0.28[d]	1.61 ± 0.30[d]	1.55 ± 0.36[c]	2.31 ± 0.36[d]
BUN (mg/dl)	20 ± 1	18 ± 1	18 ± 1	21 ± 1		21 ± 1	19 ± 1	21 ± 1	21 ± 2		21 ± 1	20 ± 1	21 ± 1	22 ± 1	
S-Cr (mg/dl)	0.43 ± 0.01[b]	0.39 ± 0.01[a]	0.36 ± 0.01	0.46 ± 0.02		0.36 ± 0.01	0.35 ± 0.01	0.34 ± 0.02	0.44 ± 0.01		0.35 ± 0.01	0.38 ± 0.02	0.43 ± 0.02[b]	0.45 ± 0.02	
Ccr (ml/min)	2.43 ± 0.09	3.08 ± 0.16[b]	3.54 ± 0.21[b]	3.00 ± 0.17[c]		2.19 ± 0.04	2.34 ± 0.16	2.71 ± 0.24	2.10 ± 1.10		2.37 ± 0.11	2.28 ± 0.16	2.27 ± 0.10	2.19 ± 0.08	
S-Na (mmol/l)	137.2 ± 0.5[c]	135.3 ± 0.1[c]	136.5 ± 0.24[c]	139.0 ± 0.4[c]		140.7 ± 0.5	138.0 ± 0.5	138.5 ± 0.2	144.0 ± 0.9		139.8 ± 0.4	137.1 ± 0.3	139.9 ± 0.4[b]	141.9 ± 0.7	
S-K (mmol/l)	5.73 ± 0.08[d]	4.84 ± 0.16[c]	4.54 ± 0.09[d]	4.52 ± 0.06[b]		4.98 ± 0.02	4.13 ± 0.03	3.73 ± 0.06	3.63 ± 0.15		5.31 ± 0.11[a]	4.16 ± 0.08	3.67 ± 0.07	4.19 ± 0.23[a]	
S-Cl (mmol/l)	100.4 ± 0.1[a]	98.5 ± 0.3	99.5 ± 0.2	100.1 ± 0.4[b]		102.3 ± 0.7	100.0 ± 1.2	99.5 ± 0.3	102.6 ± 0.6		102.3 ± 0.4	98.5 ± 0.6	101.1 ± 0.3[c]	102.0 ± 0.6	
S-Ca (mg/dl)					10.9 ± 0.1					10.5 ± 0.3					10.9 ± 0.2
S-P (mg/dl)					7.26 ± 0.54					6.60 ± 0.30					7.90 ± 0.61
T-C (mg/dl)					171 ± 9					187 ± 30					204 ± 14
HDL-C (mg/dl)					40 ± 1					36 ± 6					36 ± 3
TG (mg/dl)					239 ± 47					259 ± 52					214 ± 22
U-IS (mg/day)	3.15 ± 0.27[a]	3.10 ± 0.15	2.39 ± 0.08	2.70 ± 0.18		2.40 ± 0.22	2.47 ± 0.21	2.05 ± 0.16	2.20 ± 0.19		2.68 ± 0.12	20.91 ± 3.44[d]	32.88 ± 5.36[d]	32.41 ± 8.88[b]	
U-protein (mg/day)	13.5 ± 1.3[b]	36.2 ± 3.8	98.3 ± 4.8	150.3 ± 11.4		40.8 ± 4.2	33.0 ± 5.0	74.2 ± 12.7	161.4 ± 49.6		37.8 ± 6.3	51.1 ± 9.1	128.0 ± 23.1[a]	168.4 ± 32.1	
U-volume (ml/day)	18.8 ± 3.5	22.1 ± 2.8	21.7 ± 2.5	22.9 ± 2.9		22.5 ± 5.0	11.6 ± 3.3	14.5 ± 3.5	39.8 ± 14.0		19.9 ± 3.0	15.0 ± 3.2	25.1 ± 4.2	47.3 ± 7.1	
U-Cr (mg/day)	14.9 ± 0.5[d]	17.4 ± 0.7[d]	18.4 ± 0.7[d]	19.8 ± 0.6[d]		11.4 ± 0.3	11.6 ± 0.9	13.0 ± 0.7	13.4 ± 0.5		11.7 ± 0.4	12.3 ± 0.6	13.8 ± 0.4	14.0 ± 0.4	
U-Na (mmol/day)	17.0 ± 2.9[b]	17.4 ± 2.2	20.6 ± 3.3[a]	20.6 ± 3.0[a]		126.6 ± 31.3	76.1 ± 26.4	107.7 ± 26.0	285.2 ± 97.0		107.1 ± 17.1	81.7 ± 19.5	186.4 ± 30.8[a]	219.0 ± 73.3	
U-K (mmol/day)	46.8 ± 1.0[a]	43.5 ± 1.7[b]	36.2 ± 2.0	50.7 ± 1.3[a]		36.2 ± 2.5	23.6 ± 3.6	27.0 ± 4.3	37.8 ± 4.2		36.9 ± 3.0	28.2 ± 4.7	37.5 ± 3.8	42.4 ± 5.0	
U-Cl (mmol/day)	34.7 ± 3.5[b]	31.3 ± 3.3	31.5 ± 4.2	37.0 ± 3.5[a]		200.7 ± 47.4	121.5 ± 42.9	174.3 ± 42.9	472.1 ± 161.6		168.2 ± 26.7	130.7 ± 32.9	279.6 ± 63.4	360.4 ± 118.8	
U-Ca (mg/day)	0.58 ± 0.10[b]	0.62 ± 0.08	0.92 ± 0.09	2.12 ± 0.24	1.86 ± 0.28[a]	1.64 ± 0.20	1.24 ± 0.41	2.50 ± 0.67	5.62 ± 1.84	8.12 ± 1.62	1.68 ± 0.22	2.07 ± 0.44	5.02 ± 0.60[b]	6.10 ± 1.26	12.37 ± 2.68

All results are expressed as mean ± SE. [a] $P < 0.05$; [b] $P < 0.01$; [c] $P < 0.001$; [d] $P < 0.0001$ by Fisher's LSD test (ANOVA) as compared with DS at the same week.

DR: Dahl salt-resistant rats, DS: Dahl salt-sensitive rats, DS-IS: indoxyl sulphate-administered Dahl salt-sensitive rats.

BW: body weight, BP: blood pressure, S: serum, IS: indoxyl sulphate, BUN: blood urea nitrogen, Cr: creatinine, Ccr: creatinine clearance, T-C: total cholesterol, HDL-C: high-density lipoprotein cholesterol, TG: triglyceride, U: urine.
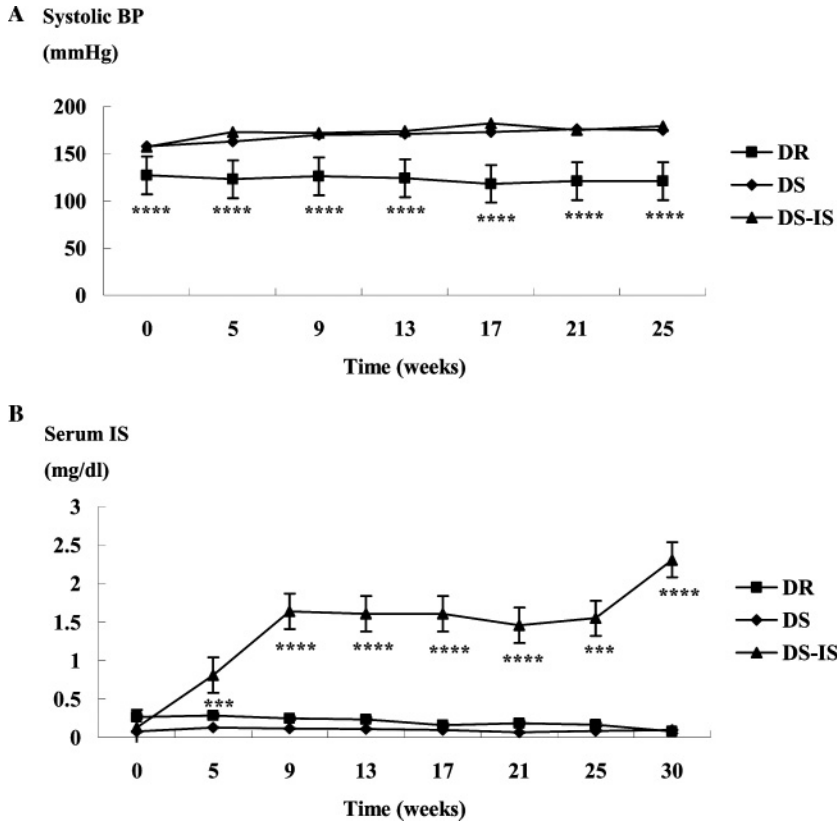
Fig. 1. Time course of systolic BP and serum IS in DR, DS and DS-IS rats. ***$P < 0.001$, ****$P < 0.0001$ vs. DS.
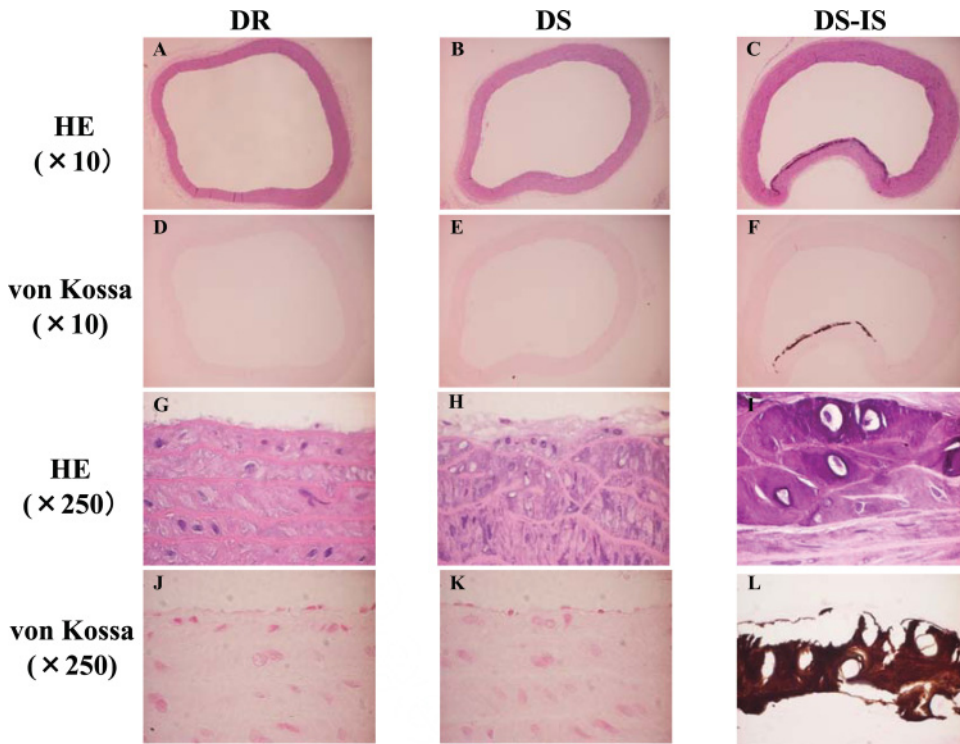

Fig. 2. H&E and von Kossa staining of arcuate aorta in DR, DS and DS-IS rats.

A

B

C

D

E

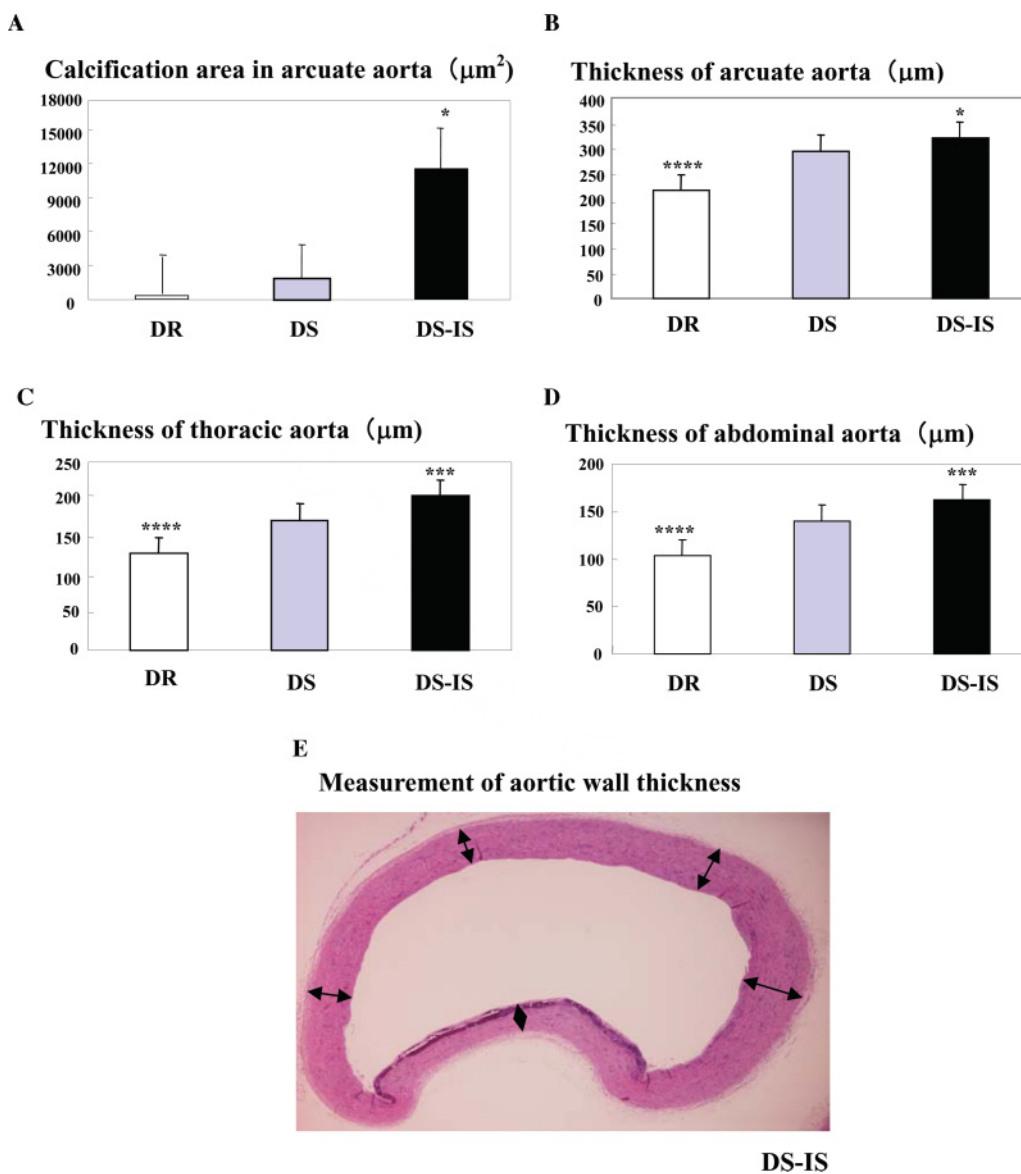## Measurement of aortic wall thickness

DS-IS

Fig. 3. Calcification area in arcuate aorta (*A*), wall thickness of the arcuate (*B*), thoracic (*C*), and abdominal aortas (*D*) in DR, DS and DS-IS rats, and the measurement of aortic wall thickness (*E*). Average of five measurements was considered representative of each rat. *$P < 0.05$, ***$P < 0.001$, ****$P < 0.0001$ vs. DS.

detected positively by von Kossa staining. Severe vascular calcification was detected in the arcuate aorta in all the six DS-IS rats, whereas it was hardly detected in DR or DS rats. H&E staining indicates that there are cells embedded in the calcification area.

Figure 3A shows the calcification area in the arcuate aorta section of rats. The calcification area was significantly and markedly increased in DS-IS rats as compared with DS rats. Figure 3 (B–D) shows wall thickness of the arcuate aorta, thoracic aorta and abdominal aortas. DS-IS rats showed significantly increased wall thickness of the arcuate aorta, thoracic aorta and abdominal aortas as compared to the DS rats. Thus, administration of IS significantly increased not only aortic calcification in the arcuate aorta, but also aortic wall thickening in the arcuate, thoracic and abdominal aortas.

Immunostaining of osteopontin, Cbfal, ALP and osteocalcin in arcuate aorta

Figure 4 shows immunostaining of osteopontin, Cbfal, ALP and osteocalcin in the arcuate aorta of DR, DS and DS-IS rats. Osteopontin, Cbfal, ALP and osteocalcin, proteins specific to osteoblasts, were colocalised in the cells embedded in the calcification area of the arcuate aorta in DS-IS rats, but not in the arcuate aorta of DR or DS rats. Negative controls stained without the primary antibodies showed no positive staining in the aorta.

Immunostaining of IS, rOAT1, rOAT3, SMA and macrophages in arcuate aorta

Figure 5 shows immunostaining of IS, rOATl, rOAT3, SMA and macrophages in the arcuate aorta of DR, DS and
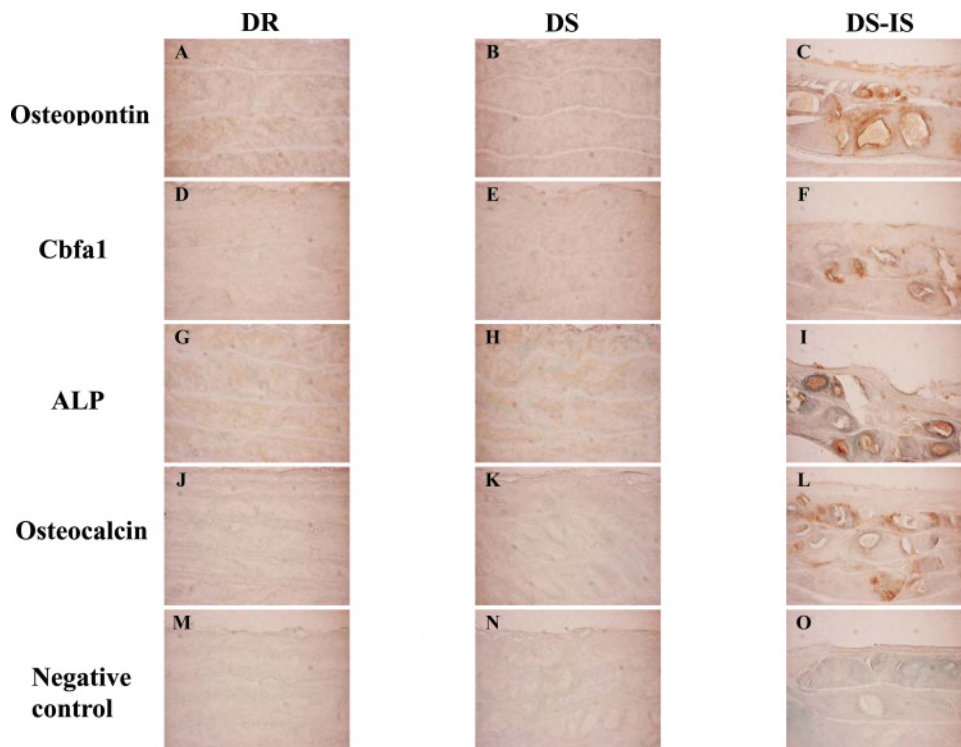
Fig. 4. Immunostaining of osteopontin, Cbfal, ALP and osteocalcin in the arcuate aorta of DR, DS and DS-IS rats (×250).
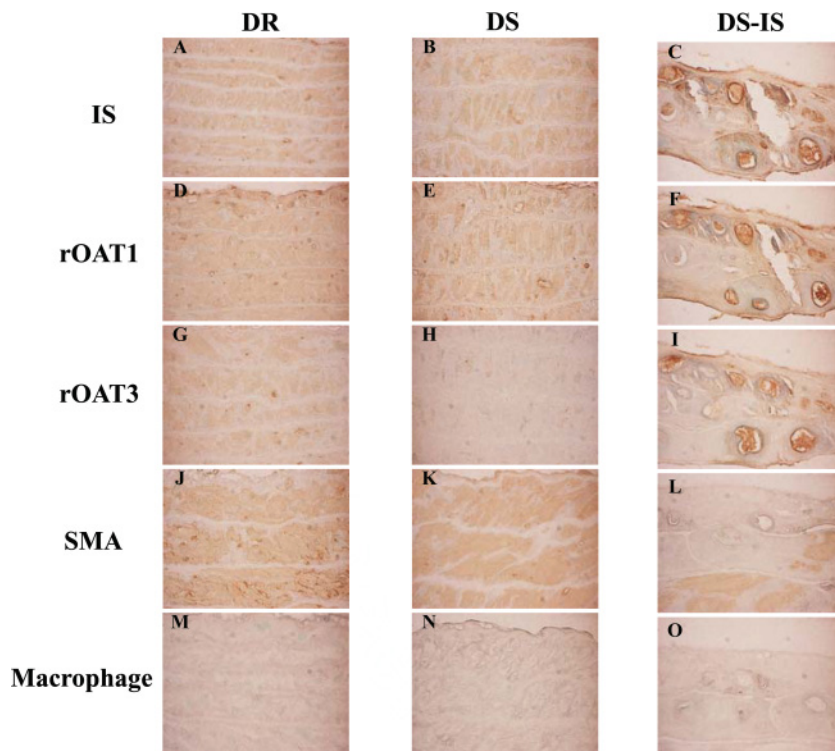

Fig. 5. Immunostaining of IS, rOATl, rOAT3, SMA and macrophages in the arcuate aorta of DR, DS and DS-IS rats (×250).
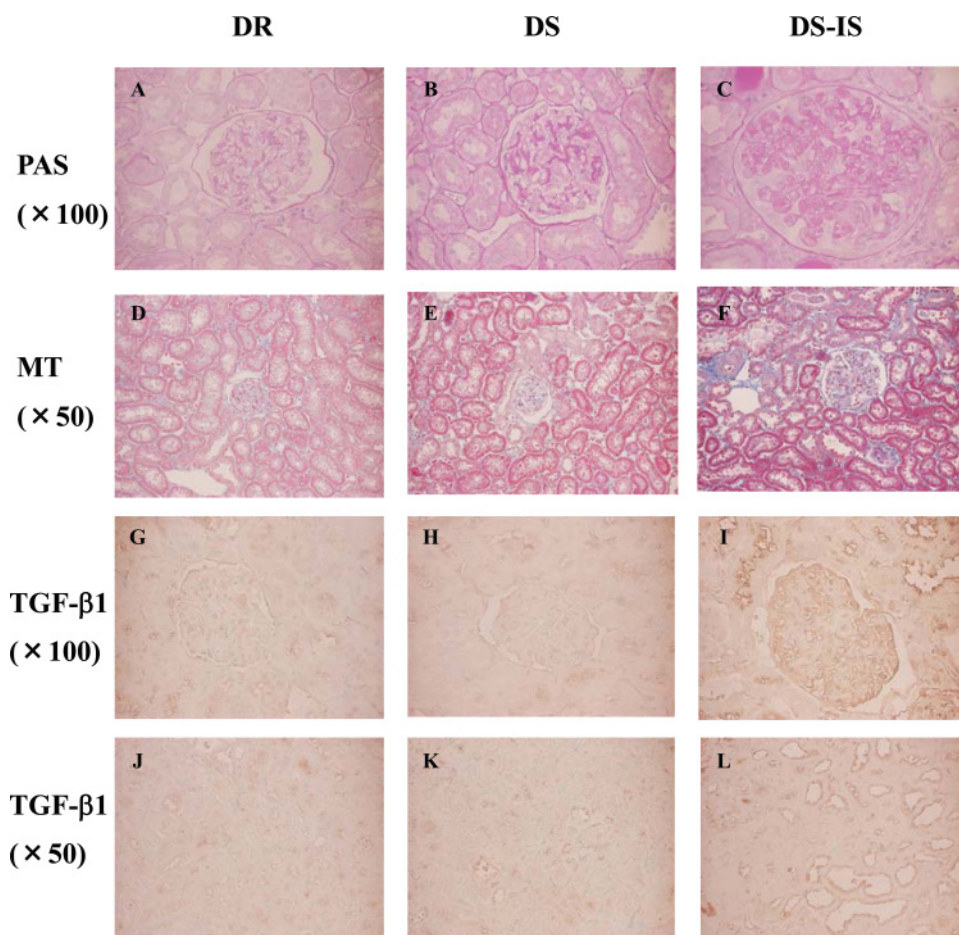
Fig. 6. PAS and Masson trichrome (MT) staining, and immunostaining of TGF-ßl in the kidneys of DR, DS, and DS-IS rats.

DS-IS rats. The cells with expression of osteoblast-specific proteins, surrounded by calcification area in the DS-IS rat showed positive staining for IS, rOATl and rOAT3, but not for SMA or macrophages. The staining of rOATl was not so prominent as compared with rOAT3. SMA is a specific protein for vascular smooth muscle cells. A loss of SMA expression in the osteoblast-like cells in the DS-IS rat supports the notion that vascular smooth muscle cells may have been transformed into osteoblasts.

Histological analysis and immunostaining of TGF-ßl in kidney

Figure 6 shows PAS and MT staining, and immunostaining of TGF-ßl in the kidneys of DR, DS, and DS-IS rats. PAS staining showed increased expansion of glomerular area and mesangial area in the DS-IS rat. MT staining showed increased interstitial fibrosis in the DS-IS rat. Immunostaining of TGF-ßl showed increased expression of TGF-ßl in the glomerulus and tubulointerstitium, especially tubular cells.

Figure 7 shows glomerular area, mesangial area, MT-positive tubulointerstitial area, TGF-ßl-positive glomerular area and TGF-ßl-positive tubulointerstitial area in the kidneys of DR, DS and DS-IS rats. DS-IS rats showed sig-

nificantly increased extent of glomerular area, mesangial area, MT-positive tubulointerstitial area and expression of glomerular and tubulointerstitial TGF-ßl as compared with DS and DR rats.

Discussion

The present study demonstrates for the first time that IS promotes aortic calcification and aortic wall thickening. Osteoblast-specific proteins, such as osteopontin, Cbfal, ALP and osteocalcin are expressed in the cells embedded in the aortic calcification area. The serum levels of IS in the DS-IS rats are around 2 mg/dl, which are comparable to, or rather below the mean serum level of IS (5.3 mg/dl) in haemodialysis patients [3,4]. Thus, IS is a vascular uraemic toxin that may be responsible, at least partially, for the progression of arteriosclerosis in CKD patients.

The pathogenesis of vascular calcification in uraemia is not yet completely understood, although increased levels of inorganic phosphate and/or uraemic toxins may play an important role by transforming vascular smooth muscle cells into osteoblast-like cells [21–24]. Vascular calcification is an active, cell-mediated process. Osteoblast differentiation factor Cbfal and several bone-associated proteins, such as
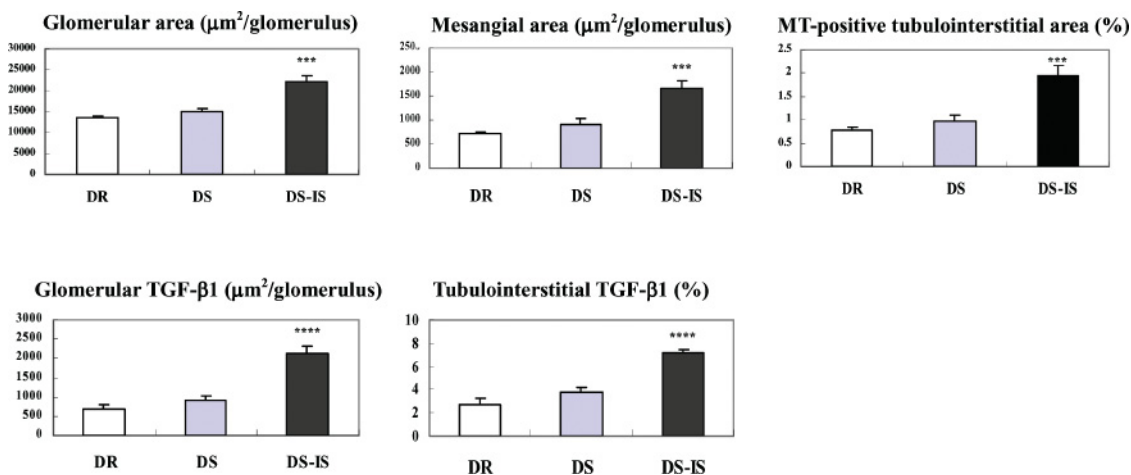
Fig. 7. Glomerular area, mesangial area, MT-positive tubulointerstitial area, TGF-ßl-positive glomerular area and TGF-ßl-positive tubulointerstitial area in the kidneys of DR, DS, and DS-IS rats. ***$P < 0.001$, ****$P < 0.0001$ vs. DS

osteopontin, ALP and osteocalcin are present in histological sections of arteries obtained from uraemic patients. High levels of inorganic phosphate and uraemic serum can transform vascular smooth muscle cells into osteoblast-like cells, possibly by upregulation of Cbfal [21–24]. Addition of ß-glycerophosphate as a donor of inorganic phosphate induced calcification and osteopontin expression in cultured vascular smooth muscle cells [21]. Addition of uraemic serum also accelerated mineralization and increased expression of Cbfal, osteopontin and ALP in cultured vascular smooth muscle cells. The uraemic serum-induced osteopontin expression in vascular smooth muscle cells is partially mediated through ALP activity and a Na/Pi co-transporter-dependent mechanism. Reduction of serum phosphorus concentration by sevelamer prevented the uraemia-enhanced arteriosclerosis and vascular calcification in the uraemic apoE-knockout mice [25]. Although there are inevitable discrepancies between rats and humans, we found *in vivo* using rats that IS may have accelerated transformation of vascular smooth muscle cells into osteoblast-like cells with expression of osteoblast-specific proteins, such as osteopontin, Cbfal, ALP and osteocalcin. Thus, we propose that IS is one of the uraemic toxins inducing osteoblast transformation of vascular smooth muscle cells.

IS, OAT1 and OAT3 were colocalized in the osteoblast-like cells embedded in the aortic calcification areas of DS-IS rats. The expression of OATs, especially OAT3 suggests that these OATs transport IS into the osteoblast-like cells, resulting in accumulation of IS within the cells, possibly followed by intracellular generation of free radicals. The finding that SMA was not colocalized in the osteoblast-like cells also supports the notion that these osteoblast-like cells lost SMA, a marker of vascular smooth muscle cells, by transformation.

In the present study, we confirmed nephrotoxicity of IS even in rats with early stage of CKD. DS-IS rats showed significantly increased extent of glomerular hypertrophy, mesangial expansion and MT-positive tubulointerstitial area with increased expression of glomerular and tubulointersti-tial TGF-ßl as compared with DS rats, although there were no significant differences in serum creatinine and creatinine clearance between the two groups. These results are consistent with our previous reports on nephrotoxicity of IS [4–8].

IS is produced in the liver from indole, a metabolite of dietary tryptophan by intestinal bacteria. An oral sorbent (AST-120) reduces serum and urine levels of IS in uraemic rats and patients with CKD stage 4 to 5 by adsorbing indole in the intestines, and consequently stimulating its excretion into faeces. AST-120 delays the progression of CKD not only in uraemic rats, but also in CKD patients [18, 26–33]. AST-120 is widely used as an approved drug not only in Japan, but also in Korea for the treatment of pre-dialysis patients with CKD stage 4 to 5 to delay the progression of CKD. A multicenter, randomized, double-blind, placebo-controlled, dose-ranging study has demonstrated that AST-120 decreased serum IS levels in a dose-dependent fashion in patients with CKD stage 4 to 5 [34]. Recently, AST-120 has been reported to reduce arterial stiffness and intima-media thickness of common carotid artery in non-diabetic pre-dialysis patients with CKD stage 4 to 5 [35]. These beneficial effects of AST-120 on arterial stiffness and intima-media thickness may be due to reduction of serum IS levels. Thus, AST-120 may also be effective in preventing aortic calcification in CKD patients by reducing the serum levels of IS.

In conclusion, IS promotes aortic wall thickening and aortic calcification with colocalization of osteoblast-specific proteins. Thus, IS is not only a nephrotoxin but also a vascular toxin, and may contribute to the progression of aortic calcification in CKD patients.

Conflict of interest statement. None declared.

References

1. Niwa T. Uraemic toxicity, indoxyl sulfate. In: Massry SG, Glassock RJ (ed.). *Textbook of Nephrology*. Baltimore, MD: Williams & Wilkins, 2001; 1269–1272

2. Niwa T. Organic acids and the uraemic syndrome: Protein metabolite hypothesis in the progression of chronic renal failure. *Semin Nephrol* 1996; 16: 167–182

3. Niwa T, Takeda N, Tatematsu A, Maeda K. Accumulation of indoxyl sulfate, an inhibitor of drug-binding, in uraemic serum as demonstrated by internal-surface reversed-phase liquid chromatography. *Clin Chem* 1988; 34: 2264–2267

4. Niwa T, Ise M. Indoxyl sulfate, a circulating uraemic toxin, stimulates the progression of glomerular sclerosis. *J Lab Clin Med* 1994; 124: 96–104

5. Niwa T, Ise M, Miyazaki T. Progression of glomerular sclerosis in experimental uraemic rats by administration of indole, a precursor of indoxyl sulfate. *Am J Nephrol* 1994; 14: 207–212

6. Miyazaki T, Ise M, Seo H, Niwa T. Indoxyl sulfate increases the gene expressions of TGF-ß$_1$, TIMP-1 and pro α(I) collagen in uraemic rat kidneys. *Kidney Int* 1997; 52: S15–S22

7. Miyazaki T, Ise M, Hirata M *et al*. Indoxyl sulfate stimulates renal synthesis of transforming growth factor-ß$_1$ and progression of renal failure. *Kidney Int* 1997; 52(S63): S211–S214

8. Enomoto A, Takeda M, Tojo A *et al*. Role of organic anion transporters in the tubular transport of indoxyl sulfate and the induction of its nephrotoxicity. *J Am Soc Nephro* 2002; 13: 1711–1720

9. Motojima M, Hosokawa A, Yamato H, Muraki T, Yoshioka T. Uraemic toxins of organic anions up-regulate PAI-1 expression by induction of NF-κB and free radical in proximal tubular cells. *Kidney Int* 2003; 63: 1671–1680

10. Foley RN, Parfrey PS, Sarnak MJ. Clinical epidemiology of cardiovascular disease in chronic renal disease. *Am J Kidney Dis* 1998; 32: S112–S119

11. Johnson DW, Craven AM, Isbel NM. Modification of cardiovascular risk in hemodialysis patients: An evidence-based review. *Hemodial Int* 2007; 11: 1–14

12. Derici U, El Nahas AM. Vascular calcifications in uraemia: Old concepts and new insights. *Semin Dial* 2006; 19: 60–68

13. Dou L, Bertrand E, Cerini C *et al*. The uraemic solutes p-cresol and indoxyl sulfate inhibit endothelial proliferation and wound repair. *Kidney Int* 2004; 65: 442–451

14. Yamamoto H, Tsuruoka S, Ioka T *et al*. Indoxyl sulfate stimulates proliferation of rat vascular smooth muscle cells. *Kidney Int* 2006; 69: 1780–1785

15. Takeda N, Niwa T, Maeda K *et al*. A rapid assay for indoxyl sulfate in uraemic serum by internal-surface reversed phase high-performance liquid chromatograph. *J Chromatosr B* 1988; 431: 418–423

16. Niwa T, Takeda N, Tatematsu A *et al*. Accumulation of indoxyl sulfate, an inhibitor of drug-binding, in uraemic serum as demonstrated by internal-surface reversed-phase liquid chromatograph. *Clin Chem* 1988; 34: 2264–2267

17. Mizobuchi M, Ogata H, Hatamura I *et al*. Up-regulation of Cbfal and Pit-1 in calcified artery of uraemic rats with severe hyperphosphataemia and secondary hyperparathyroidism. *Nephrol Dial Transplant* 2006; 21: 911–916

18. Miyazaki T, Aoyama I, Ise M, Seo H, Niwa T. An oral sorbent reduces overload of indoxyl sulfate and gene expression of TGF-ß$_1$ in uraemic rat kidneys. *Nephrol Dial Transplant* 2000; 15: 1773–1781

19. Tojo A, Sekine T, Nakajima N *et al*. Immunohistochemical localization of multispecific renal organic anion transporter 1 in rat kidney. *J Am Soc Nephrol* 1999; 10: 464–471

20. Kojima R, Sekine T, Kawachi M, Cha SH, Suzuki Y, Endou H. Immunolocalization of multispecific organic anion transporters, OAT1, OAT2, and OAT3, in rat kidney. *J Am Soc Nephrol* 2002; 13: 848–857

21. Chen NX, O'Neill KD, Duan D, Moe SM. Phosphorus and uraemic serum up-regulate osteopontin expression in vascular smooth muscle cells. *Kidney Int* 2002; 62: 1724–1731

22. Moe SM, Duan D, Doehle BP, O'Neill KD, Chen NX. Uraemia induces the osteoblast differentiation factor Cbfal in human blood vessels. *Kidney Int* 2003; 63: 1003–1011

23. Chen NX, Moe SM. Vascular calcification in chronic kidney disease. *Semin Nephrol* 2004; 24: 61–68

24. Chen NX, Duan D, O'Neill KD *et al*. The mechanisms of uraemic serum-induced expression of bone matrix proteins in bovine vascular smooth muscle cells. *Kidney Int* 2006; 70: 1046–1053

25. Phan O, Ivanovski O, Nguyen-Khoa T *et al*. Sevelamer prevents uraemia-enhanced atherosclerosis progression in apolipoprotein E-deficient mice. *Circulation* 2005; 112: 2875–2882

26. Aoyama I, Miyazaki T, Takayama F *et al*. Oral adsorbent ameliorates renal TGF-ß$_1$ expression in hypercholesterolemic rats. *Kidney Int* 1999; 56(S71): S193–S197

27. Aoyama I, Shimokata K, Niwa T. Oral adsorbent AST-120 ameliorates interstitial fibrosis and transforming growth factor-ß$_1$ expression in spontaneously diabetic (OLETF) rats. *Am J Nephrol* 2000; 20: 232–241

28. Aoyama I, Niwa T. An oral adsorbent ameliorates renal overload of indoxyl sulfate and progression of renal failure in diabetic rats. *Am J Kidney Dis* 2001; 37: S7–S12

29. Aoyama I, Shimokata K, Niwa T. Combination therapy with benazepril and oral adsorbent ameliorates progressive renal fibrosis in uraemic rats. *Nephron* 2002; 90: 297–312

30. Aoyama I, Shimokata K, Niwa T. An oral adsorbent down-regulates renal expression of genes that promote interstitial inflammation and fibrosis in diabetic rats. *Nephron* 2002; 92: 635–651

31. Aoyama I, Enomoto A, Niwa T. Effects of oral adsorbent on gene expression profile in uraemic rat kidney: cDNA array analysis. *Am J Kidney Dis* 2003; 41: S8–S14

32. Taki K, Niwa T. Indoxyl sulfate-lowering capacity of oral sorbents affects the prognosis of kidney function and oxidative stress in chronic kidney disease. *J Ren Nutr* 2007; 17: 48–52

33. Niwa T, Nomura T, Sugiyama S, Miyazaki T, Tsukushi S, Tsutsui S. The protein metabolite hypothesis, a model for the progression of renal failure: An oral adsorbent lowers indoxyl sulfate levels in undialyzed uraemic patients. *Kidney Int* 1997; 52: S23–S28

34. Schulman G, Agarwal R, Acharya M, Berl T, Blumenthal S, Kopyt N. A multicenter, randomised, double-blind, placebo-controlled, dose-ranging study of AST-120 (Kremezin) in patients with moderate to severe CKD. *Am J Kidney Dis* 2006; 47: 565–577

35. Nakamura T, Kawagoe Y, Matsuda T *et al*. Oral adsorbent AST-120 decreases carotid intima-media thickness and arterial stiffness in patients with chronic renal failure. *Kidney Blood Press Res* 2004; 27: 121–126